

Immuno-PET Imaging and Radioimmunotherapy of ^{64}Cu -/ ^{177}Lu -Labeled Anti-EGFR Antibody in Esophageal Squamous Cell Carcinoma Model

In Ho Song^{1,2}, Tae Sup Lee¹, Yong Serk Park², Jin Sook Lee³, Byung Chul Lee⁴, Byung Seok Moon⁴, Gwang Il An¹, Hae Won Lee⁵, Kwang Il Kim¹, Yong Jin Lee¹, Joo Hyun Kang¹, and Sang Moo Lim^{1,6}

¹Molecular Imaging Research Center, Korea Institute of Radiological and Medical Sciences (KIRAMS), Seoul, South Korea;

²Department of Biomedical Laboratory Science, Yonsei University, Wonju, South Korea; ³Department of Anatomy, Yonsei University Wonju Collage of Medicine, Wonju, South Korea; ⁴Department of Nuclear Medicine, Seoul National University Bundang Hospital, Seoul National University College of Medicine, Seongnam, South Korea; ⁵Department of Thoracic Surgery, KIRAMS, Seoul, South Korea; and ⁶Department of Nuclear Medicine, KIRAMS, Seoul, South Korea

Key Words: cetuximab; ^{64}Cu ; immuno-PET; ^{177}Lu ; radioimmunotherapy

J Nucl Med 2016; 57:1105–1111

DOI: 10.2967/jnumed.115.167155

Immuno-PET provides valuable information about tumor location, phenotype, susceptibility to therapy, and treatment response, especially to targeted radioimmunotherapy. In this study, we prepared antiepidermal growth factor receptor (EGFR) antibody via identical chelator, 3,6,9,15-tetraazabicyclo[9.3.1]-pentadeca-1(15),11,13-triene-3,6,9-triacetic acid (PCTA), labeled with ^{64}Cu or ^{177}Lu to evaluate the EGFR expression levels using immuno-PET and the feasibility of radioimmunotherapy in an esophageal squamous cell carcinoma (ESCC) model. **Methods:** Cetuximab was conjugated with *p*-SCN-Bn-PCTA and radiolabeled with ^{64}Cu or ^{177}Lu . In vitro EGFR expression levels were determined and compared using flow cytometry and cell binding assay. In vivo EGFR expression levels were evaluated via immuno-PET imaging of ^{64}Cu -cetuximab and biodistribution analysis. Micro-SPECT/CT imaging, biodistribution, and radioimmunotherapy studies of ^{177}Lu -cetuximab were performed in the ESCC model. Therapeutic responses were monitored using ^{18}F -FDG PET and immunohistochemical staining. **Results:** ^{64}Cu - or ^{177}Lu -labeled antibodies showed high radiolabeling yield (>98%), stability (>90%), and favorable immunoreactivity. In vitro EGFR status measured by cell binding assay was correlated with the flow cytometry data. Immuno-PET, micro-SPECT/CT, and biodistribution demonstrated specific uptake in ESCC tumors depending on the EGFR expression levels. Tumor accumulation of ^{64}Cu - and ^{177}Lu -cetuximab was peaked at 48 and 120 h, respectively. Radioimmunotherapy with ^{177}Lu -cetuximab showed significant inhibition of tumor growth ($P < 0.01$) and marked reduction of ^{18}F -FDG SUV compared with that of control ($P < 0.05$). Terminal deoxynucleotidyl transferase dUTP nick-end labeling positivity and Ki-67 staining indices increased and decreased, respectively, in the radioimmunotherapy group compared with other groups ($P < 0.01$). **Conclusion:** ^{64}Cu -cetuximab immuno-PET represented EGFR expression levels in ESCC tumors, and ^{177}Lu -cetuximab radioimmunotherapy effectively inhibited the tumor growth. The diagnostic and therapeutic convergence radiopharmaceutical ^{64}Cu -/ ^{177}Lu -PCTA-cetuximab may be useful as a diagnostic tool in patient selection and a potent radioimmunotherapy agent in EGFR-positive ESCC tumors.

Esophageal cancer is an aggressive disease with high incidence and mortality rates (1). Two major histologic types of esophageal cancer have been defined: esophageal squamous cell carcinoma (ESCC) and esophageal adenocarcinoma. Most patients in Asia (e.g., Japan and China) have ESCC (2). Despite significant improvements in diagnosis and treatment including surgical resection, chemotherapy, and radiotherapy, the 5-y survival rate remains below 15% (1). Therefore, novel therapeutic strategies are needed. In this effort, molecule-targeted therapy—especially therapy targeting the EGFR family, such as small-molecule inhibitors of tyrosine kinases and monoclonal antibodies—has been investigated in preclinical and clinical studies (3,4).

Immuno-PET is a noninvasive quantitative imaging method for obtaining comprehensive information about the targeted molecules and might be valuable for selection of patient candidates for radioimmunotherapy. Immuno-PET might provide a promising strategy for evaluating EGFR expression levels in tumors and predicting tumor response to anti-EGFR-targeted therapy. ^{64}Cu -labeled cetuximab as an immuno-PET imaging agent has been evaluated in several tumor-bearing mouse models (5,6).

Radioimmunotherapy is a targeted therapy that has the potential to enhance the efficacy of conventional monoclonal antibodies (7). Currently, ^{90}Y and ^{177}Lu have been the most frequently used radionuclides in radioimmunotherapy. Especially, ^{177}Lu is suitable for therapeutic purposes because of the low tissue penetration range (~2 mm) that is favored in treatment of small tumors while limiting irradiation of normal tissue. Additionally, ^{177}Lu emits γ -radiation with energy suitable for scintigraphy such as SPECT imaging. Because of its proper characteristics, ^{177}Lu is increasingly used in preclinical and clinical studies (8–10).

This study was aimed to investigate a convergence radiopharmaceutical, which used ^{64}Cu for a diagnostic agent or ^{177}Lu for a therapeutic agent via the same bifunctional chelating agent, 3,6,9,15-tetraazabicyclo[9.3.1]-pentadeca-1(15),11,13-triene-3,6,9-triacetic

Received Sep. 30, 2015; revision accepted Feb. 10, 2016.

For correspondence contact: Tae Sup Lee, Molecular Imaging Research Center & Research Center for Radio-Senescence, KIRAMS, 75, Nowon-gil, Nowon-gu, Seoul, 01812, South Korea.

E-mail: nobelcow@kirams.re.kr

Published online Feb. 25, 2016.

COPYRIGHT © 2016 by the Society of Nuclear Medicine and Molecular Imaging, Inc.

acid (PCTA). To accomplish this, we prepared PCTA-conjugated anti-EGFR antibodies labeled with either ^{64}Cu or ^{177}Lu . Herein, we report a convergence radiopharmaceutical using PCTA for immuno-PET imaging and radioimmunotherapy in an ESCC model.

MATERIALS AND METHODS

Cell Culture

ESCC cell lines TE-1, TE-4, TE-5, and TE-8 were obtained from RIKEN Bioresource Center Cell Bank and grown in RPMI 1640 medium. A431 (human epidermoid carcinoma) and U87MG (human glioblastoma) were purchased from American Type Culture Collection and maintained in Dulbecco modified Eagle medium. All media were supplemented with 10% fetal bovine serum and 1% antibiotics/antimycotics. Cultures were maintained at 37°C in 5% carbon dioxide incubator.

Flow Cytometry

Cells were incubated with cetuximab (Merck KGaA) or isotype control antibody (Rituximab; Roche) for 1 h at 4°C. After being washed twice with phosphate-buffered saline containing 1% bovine serum albumin (Sigma-Aldrich), the cells were incubated with fluorescein isothiocyanate-conjugated antihuman IgG (Sigma-Aldrich) for 1 h at 4°C. Stained cells were analyzed using FACS Calibur and CellQuest software (BD Immunocytometry System).

Preparation of PCTA-Cetuximab Immunoconjugate

Cetuximab was buffer-exchanged and concentrated to 10 mg/mL in 0.1 M sodium bicarbonate buffer, pH 8.5, using Vivaspinn-20 ultracentrifugation tubes (Sartorius). A 10-fold molar excess of *p*-SCN-Bn-PCTA (Macrocyclics) in dimethyl sulfoxide was added to the antibody in 0.1 M sodium bicarbonate buffer, pH 8.5. Conjugation was allowed to proceed at room temperature for 2 h and continued at 4°C overnight. Unconjugated chelator was removed by dialysis. The immunoconjugate was finally concentrated to 2 mg/mL in 20 mM sodium acetate buffer, pH 6.5. To determine the number of chelates per antibody, mass spectrometry was performed.

Radiolabeling

^{64}Cu was produced at KIRAMS by 50-MeV cyclotron irradiation (11). ^{177}Lu was purchased from ITM AG. $^{64}\text{CuCl}_2$ (74 MBq) or $^{177}\text{LuCl}_3$ (74–740 MBq) was added to 1 mg of PCTA-cetuximab. The reaction mixtures were incubated for 1 h at room temperature or 37°C, respectively, with constant shaking. Radiolabeling yield and purity were assessed by instant thin-layer chromatography silica gel (Pall Corp.) as the stationary phase and 20 mM citrate buffer, pH 5, with 50 mM ethylenediaminetetraacetic acid as the mobile phase. Radiochemical purity was analyzed by size-exclusion high-performance liquid chromatography.

In Vitro Cell Binding Assay

Cell binding studies with ^{64}Cu -/ ^{177}Lu -radiolabeled antibody were performed using A431, U87MG, TE-1, TE-4, TE-5, and TE-8 cells (1×10^6 cells/tube, triplicate). Nonspecific binding was determined in the presence of 100-fold-excess of cetuximab. After incubation, the samples were washed twice in cold phosphate-buffered saline containing 1% bovine serum albumin. Each sample was counted in a γ -counter (Wizard 1480; Perkin-Elmer). Cell bound radioactivity (%) was calculated using (cell bound radioactivity – nonspecific binding radioactivity)/total radioactivity $\times 100$.

Cytotoxicity Assay of ^{177}Lu -PCTA-Cetuximab

TE-4 and TE-8 cells (5×10^4) were treated with ^{177}Lu -PCTA-cetuximab at 0.037, 0.37, 0.74, and 1.48 MBq/well. Control wells were treated with medium alone and unlabeled cetuximab (2 μg /well). After 1 h, the

medium was aspirated, and complete medium was added. At 3 d after treatment, the cytotoxic effects were evaluated by determining cell viability using an ADAM automated cell counter (Digital-Bio). Data were expressed as percentage of control proliferation, using the number of living cells incubated with medium alone as a control.

Animal Model

All animal experiments were done under a protocol approved by KIRAMS Institutional Animal Care and Use Committee. Female athymic BALB/c mice aged 6 wk (NARA Biotech) were injected subcutaneously with 1×10^7 TE-4 or TE-8 cells in the right flank. Biodistribution was conducted when tumors reached a long diameter of 1 cm at 3–4 wk after tumor implantation.

Biodistribution Study

Biodistribution of ^{64}Cu -PCTA-cetuximab was evaluated in TE-4 or TE-8 tumor-bearing mice. Each tumor-bearing mouse was intravenously injected with 3.7 MBq of ^{64}Cu -PCTA-cetuximab. The mice ($n = 3$ or 4/group) were sacrificed at 2, 24, 48, and 72 h after injection. In the case of ^{177}Lu -PCTA-cetuximab, biodistribution was performed in TE-8 tumor-bearing mice at 2 h and 1, 3, 5, 7, and 14 d after injection. The mice ($n = 4$ /group) were intravenously administered 12.95 MBq of ^{177}Lu -PCTA-cetuximab. For blocking experiments, excess cold cetuximab (2 mg/head) was intravenously injected 30 min before ^{177}Lu -PCTA-cetuximab, and the mice were sacrificed at 5 d after injection. Blood and various tissues were weighed and measured for radioactivity using a γ -counter (Wizard 1480). The accumulated activity was represented as the percentage injected radioactivity dose per a gram of tissue (%ID/g). Tumor-to-blood, tumor-to-muscle, and tumor-to-liver (T/L) ratios were calculated.

Immuno-PET Imaging

To evaluate tumor targeting of ^{64}Cu -PCTA-cetuximab and in vivo EGFR expression levels, immuno-PET imaging was performed in TE-4 or TE-8 tumor-bearing mice. ^{64}Cu -PCTA-cetuximab (3.7 MBq) was intravenously injected into the mice, and static scans were acquired for 60 min at 2, 24, 48, and 72 h after injection using a small-animal PET scanner (microPET R4; Concorde Microsystems). Quantitative data were expressed as SUV, which is defined as tissue concentration (MBq/mL)/injected dose (MBq)/the body weight (g) (12). Images were visualized using ASIPRO display software (Concorde Microsystems).

Micro-SPECT/CT Imaging

Micro-SPECT/CT was performed on days 1, 3, 7, 10, and 14 after injection of ^{177}Lu -PCTA-cetuximab (12.95 MBq). Thirty minutes before ^{177}Lu -PCTA-cetuximab injection, excess cold cetuximab (2 mg/head) was intravenously injected for blocking experiments. Imaging was performed on a NanoSPECT/CT tomograph (Bioscan Inc.) equipped with 4 NaI detectors and fitted with 1.4-mm mouse whole-body multipinhole collimators with 9 pinholes (full width at half maximum ≤ 1.2 mm). Twenty-four projections were acquired in a 256×256 acquisition matrix with 200 s per projection. Images were reconstructed using a 2-dimensional ordered-subset expectation maximization algorithm (9 iterations). Cone-beam CT images were acquired (180 projections, 1 s/projection, 45 kVp, 177 μA) before micro-SPECT imaging. Micro-SPECT and CT images were coregistered using InvivoScope software (version 2.0; Bioscan Inc.). After imaging, digital whole-body autoradiography was performed by previously described methods with minor modifications (11).

Radioimmunotherapy

TE-8 tumor-bearing mice were randomly divided into 3 groups ($n = 6$ or 7 per group). Each group was treated with a single dose of saline, cetuximab (5 mg/kg), or ^{177}Lu -labeled cetuximab (12.95 MBq). Tumor

volume was calculated by long diameter \times (short diameter)²/2, and body weight was measured 5 times a week.

Therapeutic Response Monitoring with ¹⁸F-FDG PET Imaging

To evaluate glucose metabolic change by treatment with cetuximab and radioimmunotherapy in the TE-8 model, ¹⁸F-FDG PET experiments were performed on days 7 and 14 after treatment. ¹⁸F-FDG (7.4 MBq) was injected intravenously 1 h before scanning, and static scans were obtained for 20 min. PET images were analyzed and quantified as described previously (13).

Immunohistochemistry

Tumor tissues were harvested on day 16 after treatment and immediately fixed in 4% paraformaldehyde. Apoptosis was detected using a terminal deoxynucleotidyl transferase dUTP nick-end labeling (TUNEL) assay kit (Millipore) on 4- μ m-thick sections according to the manufacturer's instructions. Tumor sections were stained with Ki-67-specific SP6 rabbit monoclonal antibody (Abcam), and the detection system EnVision+ for rabbit antibody (Dako) was applied according to the manufacturer's instructions. Counterstaining was performed with Mayer hematoxylin. Nuclear staining of Ki-67 was considered positive. In a random 6 fields, TUNEL-positive nuclei percentage and the Ki-67 staining index were defined as the percentage of positive nuclei within 800–1,000 number of nuclei.

Statistical Analysis

Quantitative data were represented as mean \pm SD, and statistical analysis was performed by 1-way ANOVA or Student *t* test using GraphPad Prism 5 (GraphPad Software). *P* values of less than 0.05 were considered statistically significant.

RESULTS

Characteristics of ⁶⁴Cu- or ¹⁷⁷Lu-PCTA-Cetuximab

The average number of chelates per cetuximab was 4.0 ± 0.4 (Supplemental Fig. 1; supplemental materials are available at <http://jnm.snmjournals.org>). ⁶⁴Cu-/¹⁷⁷Lu-PCTA-cetuximab was prepared at high radiolabeling yield and radiochemical purity ($\geq 98\%$), which was checked by instant thin-layer chromatography and size-exclusion high-performance liquid chromatography analysis (Supplemental Fig. 2). The immunoreactivity of ⁶⁴Cu- or ¹⁷⁷Lu-cetuximab was measured to be 0.972 and 0.976, respectively (Supplemental Figs. 3A and 3B). These results suggested that conjugation of PCTA and labeling of radionuclides to cetuximab did not reduce the binding ability of the antibody. The radioimmunoconjugates showed high stabilities in serum at 37°C for 24 h ($90.1\% \pm 0.6\%$) and 7 d ($90.6\% \pm 0.4\%$) (Supplemental Figs. 3C and 3D).

Characterization of EGFR Expression in ESCC

Relative expression levels of EGFR in 4 ESCC cell lines were determined by flow cytometry (Fig. 1A). The TE-8 cell line expressed a relatively high level of EGFR, and the other 3 cell lines showed intermediate EGFR expression.

The EGFR expression levels obtained from flow cytometry were compared with cell binding assay, performed using ⁶⁴Cu- or ¹⁷⁷Lu-PCTA-cetuximab. A431 and U87MG were used as positive and negative controls, respectively. Cell bound radioactivity (%) of ⁶⁴Cu-PCTA-cetuximab in ESCC cell lines was the highest in TE-8 cells ($70.9\% \pm 1.5\%$), moderate in TE-1 ($42.0\% \pm 0.5\%$) and TE-5 ($42.7\% \pm 0.3\%$) cells, and relatively low in TE-4 cells ($15.2\% \pm 0.3\%$) (Fig. 1B). The cell bound radioactivity of ¹⁷⁷Lu-PCTA-cetuximab showed a pattern similar to that of ⁶⁴Cu-PCTA-cetuximab. Cell binding assay could differentiate between TE-4

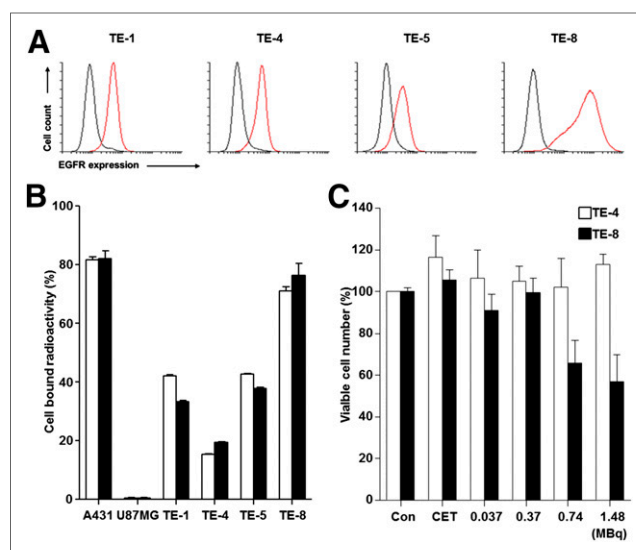


FIGURE 1. Analysis of EGFR expression and cytotoxicity of ¹⁷⁷Lu-labeled cetuximab on ESCC cell lines. (A) Flow cytometry using cetuximab. (B) Cell binding assay of ⁶⁴Cu-/¹⁷⁷Lu-PCTA-cetuximab. (C) Cytotoxicity of ¹⁷⁷Lu-PCTA-cetuximab. CET = cetuximab; Con = control.

and TE-1 or TE-5 in EGFR expression level, but flow cytometry analysis could not. The difference may be due to the sensitivity of the analytic method.

Cytotoxicity of ¹⁷⁷Lu-Cetuximab in ESCC Cells

Cell viabilities after treatment with different radioactivity doses of ¹⁷⁷Lu-cetuximab are presented in Figure 1C. At a dose of 1.48 MBq, the percentage of surviving cells decreased to $56.8\% \pm 13.0\%$ in TE-8 cells (triplicate). ¹⁷⁷Lu-cetuximab showed a radioactivity dose-dependent increase in cytotoxicity, which was most significant at the 1.48 MBq/well relative to control or cetuximab-treated cells (*P* < 0.0001). Cytotoxicity was negligible in ¹⁷⁷Lu-cetuximab-treated TE-4 cells.

Biodistribution

Biodistribution data of ⁶⁴Cu-PCTA-cetuximab in TE-4 and TE-8 models are compared and summarized in Supplemental Table 1. The uptake of ⁶⁴Cu-cetuximab in major organs and tissues was similar in both tumor models. The radioactivities in blood and liver were high at 2 h, but gradually decreased over time. Liver uptake of ⁶⁴Cu-cetuximab was the highest in normal organs. The uptake of ⁶⁴Cu-cetuximab in TE-4 and TE-8 tumors steadily increased and peaked at 48 h at 9.0 ± 0.4 and 17.5 ± 4.4 %ID/g, respectively. The uptake of ⁶⁴Cu-cetuximab in TE-8 tumors was 2.1-, 1.7-, 2.0-, and 1.3-fold higher than that in TE-4 tumors at each time point.

Biodistribution data of ¹⁷⁷Lu-PCTA-cetuximab were obtained in TE-8 tumor-bearing mice (Supplemental Table 2). The uptake of ¹⁷⁷Lu-cetuximab in TE-8 tumors peaked on day 5 at 55.7 ± 6.5 %ID/g. The radioactivity in blood was 30.2 ± 1.0 %ID/g at 2 h, followed by relatively fast clearance by the end of 14 d (0.9 ± 0.6 %ID/g). Liver uptake was higher than other organs. The uptake in other organs such as the heart, lung, kidney, stomach, intestines, bone, and muscle were relatively low. Compared with the mice injected with ¹⁷⁷Lu-cetuximab alone, the uptake of ¹⁷⁷Lu-cetuximab in TE-8 tumors markedly reduced to 20.8% on day 5 in blocking experiments (*P* < 0.001), demonstrating the specificity of EGFR targeting by ¹⁷⁷Lu-cetuximab.

Immuno-PET Imaging of ^{64}Cu -PCTA-Cetuximab

To evaluate the potential of ^{64}Cu -PCTA-cetuximab as an immuno-PET imaging agent for EGFR expression levels, we performed immuno-PET imaging in TE-4 or TE-8 xenograft models (triplicate). TE-4 and TE8 tumors were clearly visible on PET images after 24 h (Fig. 2). Physiologic liver uptake was observed in both models but gradually reduced. The SUV of ^{64}Cu -cetuximab was 1.4-fold higher in TE-8 tumors than TE-4 tumors at 48 h. T/L ratios of the TE-4 and TE-8 models at 48 h were 1.1 and 1.7, respectively. Immuno-PET images were consistent with the biodistribution data of ^{64}Cu -PCTA-cetuximab.

Micro-SPECT/CT Imaging and Digital Whole-Body Autoradiography of ^{177}Lu -PCTA-Cetuximab

Micro-SPECT/CT imaging was performed to investigate the *in vivo* behavior of ^{177}Lu -PCTA-cetuximab. Representative volume images and coronal images of TE-8 tumor-bearing mice on day 5 after injection of ^{177}Lu -cetuximab were shown in Figure 3. The TE-8 tumor was clearly visualized, and a relatively low uptake was observed in the liver. Digital whole-body autoradiography images showed a distribution pattern similar to the micro-SPECT/CT images. In the blocking experiments, tumor uptake of ^{177}Lu -cetuximab was markedly reduced by excess cold cetuximab, indicating that EGFR targeting by ^{177}Lu -cetuximab was specific.

Radioimmunotherapy

Antitumor effects of ^{177}Lu -cetuximab were assessed in TE-8 xenograft models. As shown in Figure 4, a time-dependent increase in tumor volume was observed in the saline- and cetuximab-treated groups. In contrast, ^{177}Lu -cetuximab-treated TE-8 tumor on day 16 after treatment showed a 34.3% reduction compared with that

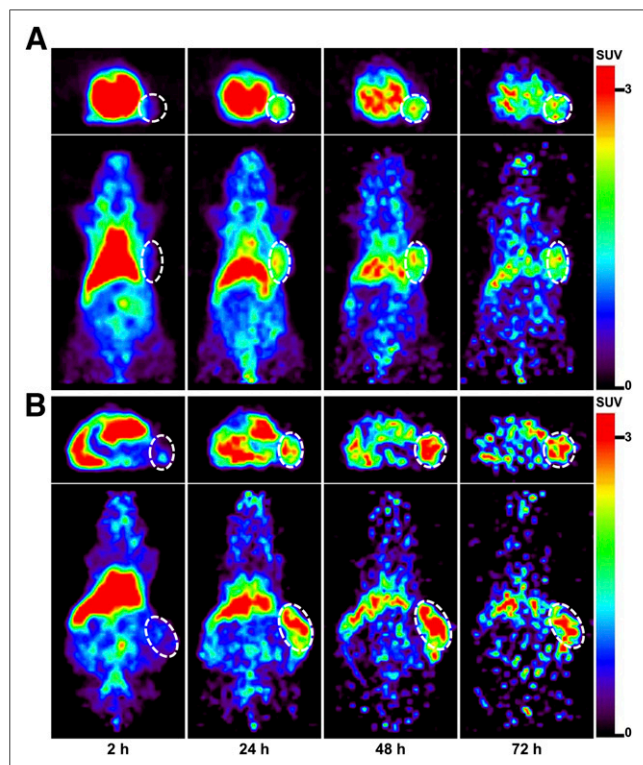


FIGURE 2. Immuno-PET images of ^{64}Cu -PCTA-cetuximab in TE-4 (A) or TE-8 (B) model at each time point. White dotted circle is tumor.

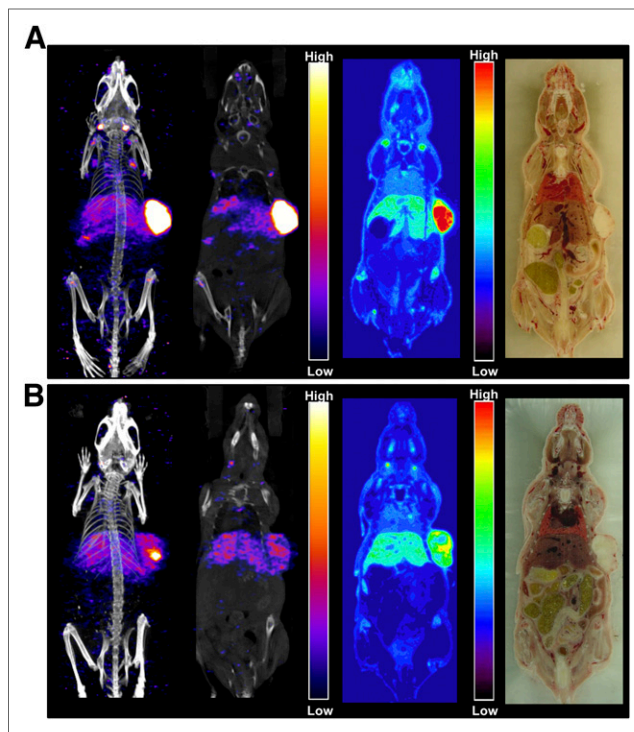


FIGURE 3. Micro-SPECT/CT and digital whole-body autoradiography images of ^{177}Lu -cetuximab without (A) and with (B) blocking (cetuximab 2 mg/head) in TE-8 models. SPECT/CT volume images (left first 2 panels) and coronal images (middle panels) were acquired on day 5 after injection. After micro-SPECT/CT scanning, digital whole-body autoradiography (third panels) and frozen photo (fourth panels) images were obtained.

on day 6 after treatment. TE-8 tumor volume in the ^{177}Lu -cetuximab-treated group showed a statistically significant difference compared with that in the saline- and cetuximab-treated groups on day 16 ($P < 0.05$). TE-8 tumor models tolerated the ^{177}Lu -cetuximab treatment, and no apparent body weight loss was observed (Supplemental Fig. 4).

Monitoring Therapeutic Efficacy by ^{18}F -FDG PET Imaging

To assess tumor response to ^{177}Lu -cetuximab therapy, ^{18}F -FDG PET imaging was performed (Fig. 5). We used the ^{18}F -FDG uptake in the saline-treated group as a baseline and compared ^{18}F -FDG uptake between saline- and cetuximab- or ^{177}Lu -PCTA-cetuximab-treated groups. There was little difference in ^{18}F -FDG uptake between saline- and cetuximab-treated groups. However, the ^{177}Lu -cetuximab-treated group (0.66 ± 0.12) showed marked reduction of ^{18}F -FDG SUV compared with that of saline-treated group (0.94 ± 0.12) on day 14 after treatment ($P < 0.05$).

Immunohistochemistry

A TUNEL assay was performed to evaluate apoptosis induced by ^{177}Lu -cetuximab treatment in TE-8 tumors. TUNEL-positive apoptotic cells were more apparent in TE-8 tumors from the ^{177}Lu -cetuximab-treated group than those from the saline- and cetuximab-treated groups (Fig. 6A). Apoptotic cells markedly increased in ^{177}Lu -cetuximab-treated TE-8 tumors (12.1 ± 2.2) compared with saline- (2.9 ± 1.3) and cetuximab- (3.9 ± 1.1) treated TE-8 tumors ($P < 0.001$), indicating that ^{177}Lu -cetuximab treatment increased apoptosis (Fig. 6C). Proliferation in TE-8

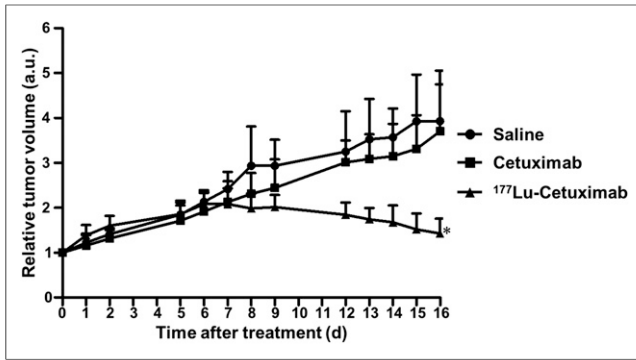


FIGURE 4. Radioimmunotherapeutic efficacy of ¹⁷⁷Lu-PCTA-cetuximab in TE-8 models. * = vs. saline- and cetuximab-treated groups, $P < 0.05$. a.u. = arbitrary unit.

xenografts was assessed by staining sections for the proliferation antigen Ki-67 (Fig. 6B). ¹⁷⁷Lu-cetuximab caused a significant decrease (45.4 ± 2.9 , $P < 0.001$) in Ki-67 staining compared with tumors treated with saline (79.2 ± 3.7) and cetuximab (82.3 ± 5.7) (Fig. 6D).

DISCUSSION

Surgery is considered as the primary treatment for patients with potentially resectable esophageal cancer without metastasis. However, most patients are diagnosed with locally advanced tumors, regional lymph node involvement, or metastatic disease (14). Clinical trials have attempted to improve the clinical outcome by reducing the rate of local disease recurrence through integrating radiotherapy and chemotherapy in patients with ESCC, but a clear benefit has never been achieved (15,16). Thus, development of

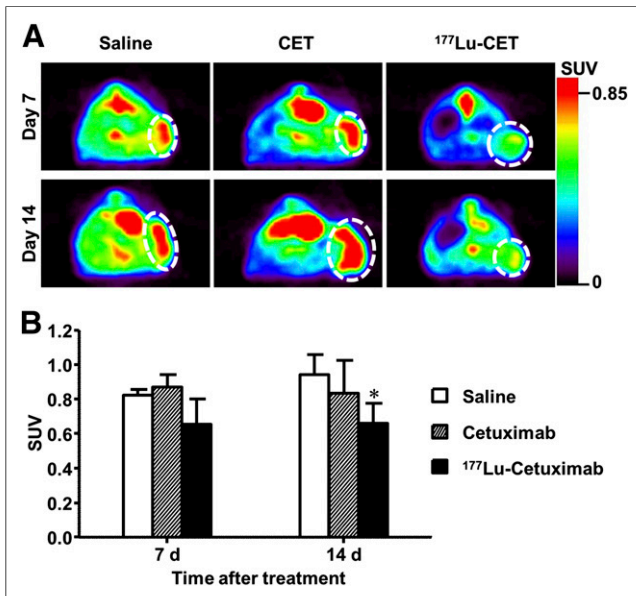


FIGURE 5. Therapeutic response monitoring of ¹⁷⁷Lu-cetuximab treatment using ¹⁸F-FDG PET in TE-8 models. (A) ¹⁸F-FDG PET images were obtained on day 7 (top) and day 14 (bottom) after treatment. (B) Quantitative ¹⁸F-FDG uptake analysis. * = vs. saline-treated group, $P < 0.05$. CET = cetuximab.

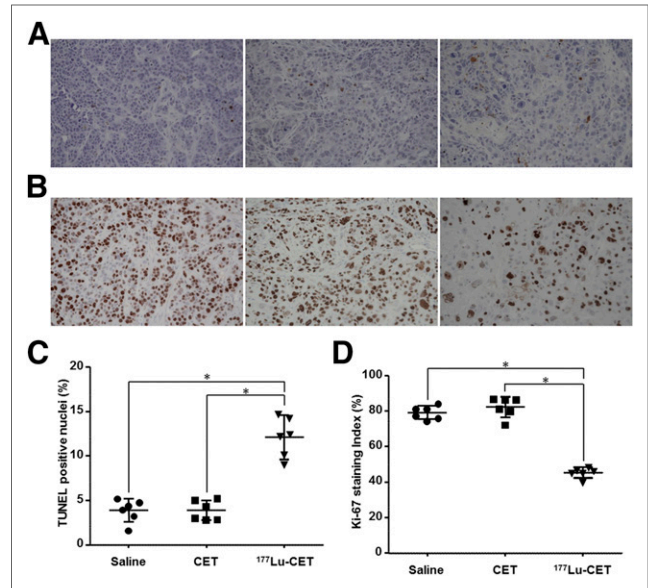


FIGURE 6. Immunohistochemical staining of TUNEL and Ki-67 in TE-8 tumors. TUNEL (A) and Ki-67 (B) staining showing positive cells were stained brown ($\times 400$ magnification). Quantitative analysis of TUNEL (C) and Ki-67 (D) staining. * $P < 0.001$. CET = cetuximab.

adequate screening techniques and effective novel therapeutic regimens are urgently needed. Recent insights into the biology of esophageal cancers have nominated potential targets for novel therapies and stratification of patient populations (17). Numerous studies have reported the high incidence of EGFR expression in ESCC, and it has been reasoned that EGFR-targeted therapy might prove an effective strategy for ESCC treatment (18,19). Immuno-PET can provide noninvasive quantitative assessment of specific molecular targets and predict whether the patients are likely to benefit from targeted therapy (20). Radioimmunotherapy could be used as an alternative therapy for patients who have failed to respond to conventional therapies. In this study, we report that ⁶⁴Cu-PCTA-cetuximab immuno-PET was useful for evaluating the levels of in vivo EGFR expression on ESCC tumors and ¹⁷⁷Lu-PCTA-cetuximab radioimmunotherapy was effective in inhibiting the growth of ESCC tumors.

⁶⁸Ga is a short-lived positron emitter (half-life, 68 min) and is readily produced from a commercially available ⁶⁸Ge/⁶⁸Ga generator. Recently, ⁶⁸Ga-based radiopharmaceuticals have been used extensively in small-size molecules such as peptides, antibody fragments, Affibody molecules, or nanobodies with faster pharmacokinetics and bioavailability (21). ⁶⁸Ga-labeled somatostatin receptor-targeting compounds have been applied for patients with neuroendocrine tumors. Because of the short half-life of ⁶⁸Ga, ⁶⁴Cu or ⁸⁹Zr seems to be used for immuno-PET imaging with fully intact antibodies.

We selected ⁶⁴Cu and ¹⁷⁷Lu for radiolabeling of cetuximab because of their favorable physical and chemical characteristics. For immuno-PET imaging, ⁶⁴Cu-labeled antibody is of particular interest because the half-life of ⁶⁴Cu (12.7 h) is suitable for targeting and clearance kinetics of antibodies (22). ¹⁷⁷Lu displays low-energy β^- -emission (497 keV, 78.7%) with minimal tissue penetration, making it suitable for therapy of small and metastatic tumors (23). To obtain antibodies radiolabeled with ⁶⁴Cu or ¹⁷⁷Lu, a proper chelator

is needed. DOTA has been widely used for labeling radiometal; however, DOTA is not ideal for radiolabeling because of slow reaction kinetics and moderate stability of the complex in vivo (22,23). Recently, various different chelators, NOTA, Oxo-DO3A, and PCTA, have been investigated for complexing ^{64}Cu (24). Similar to the literature, in our study, PCTA showed high radiolabeling yield and in vitro serum stability under mild conditions (weakly acidic pH and room temperature). ^{64}Cu - ^{177}Lu -PCTA-cetuximab did not require further purification because the radiolabeling yield and radiochemical purity were greater than 98%, respectively (Supplemental Fig. 2), and the immunoreactivity of immunoconjugates was not affected by PCTA conjugation and radiolabeling process (Supplemental Fig. 3).

In small-animal PET imaging, both TE-4 and TE-8 tumors clearly visualized and showed peaked uptake at 48 h after injection (Fig. 2). In evaluating the molecular target or patient selection using immuno-PET imaging, the absolute tumor uptake of ^{64}Cu -PCTA-cetuximab could not provide the appropriate information because both low-EGFR-expressing TE-4 and high-EGFR-expressing TE-8 showed above 9 %ID/g in tumor uptake at 48 h (Supplemental Table 1). To address whether ^{64}Cu -PCTA-cetuximab immuno-PET might select the pertinent target and predict tumor response, we compared the target-to-background ratios of ^{64}Cu -PCTA-cetuximab. Tumor-to-blood, tumor-to-muscle, and T/L ratios of TE-8 tumors at 48 h were 2.5, 1.7, and 2.4-fold higher, respectively, than the ratios of TE-4 tumors. Notably, ^{64}Cu -PCTA-cetuximab showed higher TE-8 tumor uptake than physiologic liver uptake, whereas TE-4 tumor uptake was similar to liver uptake. Therefore, the T/L ratio might be a useful criterion for target selection. Further preclinical and clinical research is required in various ESCC animal models and patients with tumors expressing varying level of EGFR to validate ^{64}Cu -PCTA-cetuximab as an imaging biomarker and to establish PET signal cutoff value for target selection.

There exists some controversy about the correlation between EGFR expression levels and uptake of radiolabeled cetuximab in tumors. EGFR expression levels were well correlated with accumulation of radiolabeled cetuximab (5), but Aerts et al. suggested that the disparity between EGFR expression levels and radiolabeled cetuximab uptake in tumors might be influenced by additional factors, such as tumor vasculature density and permeability, tumor interstitial pressure and binding site barrier, and the pharmacokinetics and tumor penetration ability of antibodies (25). Although this study was small scale, radioactivities in tumors were positively correlated with EGFR protein expression levels as measured by flow cytometry and in vitro cell binding assay (Fig. 1). For clinical translation of ^{64}Cu -cetuximab, further studies are needed in large scale using a variable ESCC xenograft model.

In general, the dose-limiting factor in radioimmunotherapy was myelotoxicity. The study of ^{177}Lu -CC49 reported that 4 of 9 tumor-bearing mice survived after 13.5 MBq, whereas all mice receiving 12.95 MBq of ^{177}Lu -CC49 survived (26). The maximal tolerated dose of ^{177}Lu -chCE7 in nude mice bearing human ovarian cancer was experimentally determined to be 12 MBq (8). In this study, the therapeutic dose of ^{177}Lu -cetuximab was determined on the basis of the literature. Though we did not evaluate hematologic toxicity, there was no evidence of body weight loss. The low bone uptake suggests that our radioimmunoconjugate is highly stable in vivo.

The term convergence radiopharmaceutical refers to an immunoconjugate containing an identical chelator that can readily be used for both imaging and therapeutic application without significant

alteration of tumor-targeting efficacy. Thus, the convergence radiopharmaceutical $^{64}\text{Cu}/^{177}\text{Lu}$ for immuno-PET imaging and radioimmunotherapy may provide a tailored medical regimen that can be specific to the individual characteristics of each patient through the visualization and quantification of target expression by immuno-PET imaging as well as selective therapeutic radiation delivery by radioimmunotherapy.

CONCLUSION

We successfully labeled anti-EGFR antibody with $^{64}\text{Cu}/^{177}\text{Lu}$ via the identical chelator, PCTA, for immuno-PET imaging and radioimmunotherapy. This study showed that ^{64}Cu -PCTA-cetuximab could be used as a surrogate PET biomarker to evaluate EGFR expression in ESCC tumors and ^{177}Lu -cetuximab has the potential to inhibit the tumor growth. Diagnostic and therapeutic convergence radiopharmaceutical $^{64}\text{Cu}/^{177}\text{Lu}$ -cetuximab may be used as a diagnostic tool for patient selection and a potent radioimmunotherapy agent in EGFR-positive ESCC tumors.

DISCLOSURE

The costs of publication of this article were defrayed in part by the payment of page charges. Therefore, and solely to indicate this fact, this article is hereby marked "advertisement" in accordance with 18 USC section 1734. This research was funded by a grant from the National R&D Program for Cancer Control, Ministry for Health and Welfare (1120260), and Nuclear Research & Development Program (no. 50526-2015 and NRF-2012M2A2A7013480) of the Ministry of Science, ICT and Future Planning, South Korea. No other potential conflict of interest relevant to this article was reported.

REFERENCES

1. Torre LA, Bray F, Siegel RL, Ferlay J, Lortet-Tieulent J, Jemal A. Global cancer statistics, 2012. *CA Cancer J Clin*. 2015;65:87–108.
2. Lin Y, Totsuka Y, He Y, et al. Epidemiology of esophageal cancer in Japan and China. *J Epidemiol*. 2013;23:233–242.
3. Enzinger PC, Mayer RJ. Esophageal cancer. *N Engl J Med*. 2003;349:2241–2252.
4. Akkili M, Ilson DH. Targeted agents and esophageal cancer: the next step? *Semin Radiat Oncol*. 2007;17:62–69.
5. Cai W, Chen K, He L, Cao Q, Koong A, Chen X. Quantitative PET of EGFR expression in xenograft-bearing mice using ^{64}Cu -labeled cetuximab, a chimeric anti-EGFR monoclonal antibody. *Eur J Nucl Med Mol Imaging*. 2007;34:850–858.
6. Niu G, Sun X, Cao Q, et al. Cetuximab-based immunotherapy and radioimmunotherapy of head and neck squamous cell carcinoma. *Clin Cancer Res*. 2010;16:2095–2105.
7. Pouget JP, Navarro-Teulon I, Bardiès M, et al. Clinical radioimmunotherapy: the role of radiobiology. *Nat Rev Clin Oncol*. 2011;8:720–734.
8. Fischer E, Grünberg J, Cohrs S, et al. L1-CAM-targeted antibody therapy and ^{177}Lu -radioimmunotherapy of disseminated ovarian cancer. *Int J Cancer*. 2012;130:2715–2721.
9. Liu Z, Ma T, Liu H, et al. ^{177}Lu -labeled antibodies for EGFR-targeted SPECT/CT imaging and radioimmunotherapy in a preclinical head and neck carcinoma model. *Mol Pharm*. 2014;11:800–807.
10. Tagawa ST, Milowsky MI, Morris M, et al. Phase II study of lutetium-177-labeled anti-prostate-specific membrane antigen monoclonal antibody J591 for metastatic castration-resistant prostate cancer. *Clin Cancer Res*. 2013;19:5182–5191.
11. Park JJ, Lee TS, Son JJ, et al. Comparison of cell-labeling methods with ^{124}I -FIAU and ^{64}Cu -PTSM for cell tracking using chronic myelogenous leukemia cells expressing HSV1-tk and firefly luciferase. *Cancer Biother Radiopharm*. 2012;27:719–728.
12. Lee J, Lee TS, Ryu J, et al. RGD peptide-conjugated multimodal NaGdF₄:Yb³⁺/Er³⁺ nanophosphors for upconversion luminescence, MR, and PET imaging of tumor angiogenesis. *J Nucl Med*. 2013;54:96–103.

13. Oh YS, Lee TS, Cheon GJ, Jang IS, Jun HS, Park SC. Modulation of insulin sensitivity and caveolin-1 expression by orchidectomy in a nonobese type 2 diabetes animal model. *Mol Med*. 2011;17:4–11.
14. Nicholson RI, Gee JM, Harper ME. EGFR and cancer prognosis. *Eur J Cancer*. 2001;37:S9–S15.
15. De Vita F, Orditura M, Martinelli E, et al. A multicenter phase II study of induction chemotherapy with FOLFOX-4 and cetuximab followed by radiation and cetuximab in locally advanced oesophageal cancer. *Br J Cancer*. 2011;104:427–432.
16. Schönnemann KR, Yilmaz M, Bjerregaard JK, Nielsen KM, Pfeiffer P. Phase II study of biweekly cetuximab in combination with irinotecan as second-line treatment in patients with platinum-resistant gastro-oesophageal cancer. *Eur J Cancer*. 2012;48:510–517.
17. Boone J, van Hillegersberg R, Offerhaus GJ, van Diest PJ, Borel Rinkes IH, Ten Kate FJ. Targets for molecular therapy in esophageal squamous cell carcinoma: an immunohistochemical analysis. *Dis Esophagus*. 2009;22:496–504.
18. Kono K, Mimura K, Fujii H, Shabbir A, Yong WP, Jimmy So A. Potential therapeutic significance of HER-family in esophageal squamous cell carcinoma. *Ann Thorac Cardiovasc Surg*. 2012;18:506–513.
19. Yamazaki M, Yamashita Y, Kubo N, et al. Concurrent biological targeting therapy of squamous cell carcinoma of the esophagus with cetuximab and trastuzumab. *Oncol Rep*. 2012;28:49–54.
20. van Dongen GA, Visser GW, Lub-de Hooge MN, de Vries EG, Perk LR. Immuno-PET: a navigator in monoclonal antibody development and applications. *Oncologist*. 2007;12:1379–1389.
21. Shetty D, Lee YS, Jeong JM. ⁶⁸Ga-labeled radiopharmaceuticals for positron emission tomography. *Nucl Med Mol Imaging*. 2010;44:233–240.
22. Sihver W, Pietzsch J, Krause M, Baumann M, Steinbach J, Pietzsch HJ. Radio-labeled cetuximab conjugates for EGFR targeted cancer diagnostics and therapy. *Pharmaceuticals (Basel)*. 2014;7:311–338.
23. Dash A, Pillai MR, Knapp FF Jr. Production of ¹⁷⁷Lu for targeted radionuclide therapy: available options. *Nucl Med Mol Imaging*. 2015;49:85–107.
24. Cooper MS, Ma MT, Sunassee K, et al. Comparison of ⁶⁴Cu-complexing bifunctional chelators for radioimmunoconjugation: labeling efficiency, specific activity, and *in vitro/in vivo* stability. *Bioconjug Chem*. 2012;23:1029–1039.
25. Aerts HJWL, Dubois L, Perk L, et al. Disparity between *in vivo* EGFR expression and ⁸⁹Zr-labeled cetuximab uptake assessed with PET. *J Nucl Med*. 2009;50:123–131.
26. Schlom J, Siler K, Milenic DE, et al. Monoclonal antibody-based therapy of a human tumor xenograft with a ¹⁷⁷lutetium-labeled immunoconjugate. *Cancer Res*. 1991;51:2889–2896.